



Parsimonious Topology Based on Frank-Kasper Polyhedra in Metal–Organic Frameworks

Soochan Lee,[○] Sungmin Lee,[○] Yuna Kwak, Masood Yousaf, Eunchan Cho, Hoi Ri Moon, Sung June Cho,* Noejung Park,* and Wonyoung Choe*



Cite This: *JACS Au* 2024, 4, 2539–2546



Read Online

ACCESS |

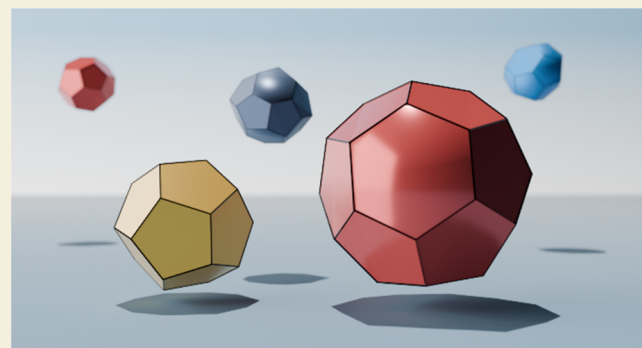
Metrics & More

Article Recommendations

Supporting Information

ABSTRACT: A new topology previously unknown in metal–organic frameworks (MOFs) provides an important clue to uncovering a new series of polyhedral MOFs. We report a novel MOF crystallized in a parsimonious **mep** topology based on Frank–Kasper (FK) polyhedra. The distribution of angles in a tetrahedral arrangement (T-O-T) is crucial for the formation of FK polyhedra in **mep** topology. This finding led us to investigate the T-O-T angle distribution in related zeolites and zeolitic imidazolate frameworks (ZIFs). Unlike zeolites, it is extremely difficult to achieve high T-O-T angles in ZIFs, which prevents the formation of some FK topologies. Density functional theory (DFT) total energy calculations support a correlation between T-O-T angles and the feasibility of new tetrahedron-based FK frameworks. This result may lead to innovative ways of accessing new cellular topologies by simple chemical tweaking of T-O-T angles.

KEYWORDS: metal–organic frameworks, topology, self-assembly, Frank–Kasper phases, polyhedra



INTRODUCTION

Metal–organic frameworks (MOFs) are becoming a central subject of materials chemistry, mainly because of a vast array of applications closely associated with their unprecedented structural diversity, as exemplified by more than 120,000 MOFs with a few thousand net topology types accumulated over the past two decades.^{1–3} Such a high degree of structural and functional tunability stems from the reticular synthesis of metal secondary building units (SBUs) and organic linkers.^{4,5} A rational synthetic strategy by careful choice of these structural building blocks can be applied to achieve a desired topology for use as a blueprint for MOF construction.^{6–9} Among these MOF structures, a rising subclass of MOFs is polyhedral MOFs in which the basic building blocks for the frameworks are polyhedra such as tetrahedra, cubes, octahedra, and cuboctahedra.^{10–13} This approach offers the potential of these geometric shapes in forming more complex and functional MOF structures.^{14,15} In contrast, MOFs based on other polyhedra are exceptionally rare. Notable examples of such underexplored MOFs are those based on four Frank–Kasper (FK) polyhedra (dodecahedron, tetradecahedron, pentadecahedron, and hexadecahedron), shown in Figure 1a.¹⁶ Originally proposed by Frank and Kasper to explain intermetallic solids (Figure 1b), these FK polyhedra are extremely versatile units capable of forming several thousand actual and hypothetical topologies.^{17–20} Particularly, one of the topologies, known as **mep** (or clathrate type I) topology, is astonishingly ubiquitous, as can

be seen in zeolites,^{21–23} gas clathrates,^{24,25} Zintl phases,^{26–30} inorganic salt,³¹ soap froth,³² metal foam,³³ and even architecture,³⁴ thus attracting intense interest in various disciplines (Figure 1c).^{35–49}

Despite the popularity of other solid-state materials, to our surprise, there is no single-crystal structure reported with **mep** topology in MOFs,² whereas another FK topology, **mtn** (or clathrate type II), is known.^{50–55} We find this missing link rather striking considering the extreme structural diversity in MOFs.⁶

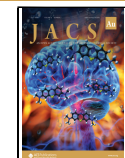
Here, we report the first example of an FK polyhedra-based MOF (FKMOF-1) crystallized in **mep** topology, together with the other (FKMOF-2) in **mtn** topology. The discovery of the unprecedented **mep** topology led us to investigate the scarcity of **mep** topology in MOFs. Notably, we have successfully implemented the reversed roles of metals and organic linkers in MOFs to stabilize **mep** topology, thereby unlocking the potential to discover topologies previously considered unachievable. This approach opens new avenues for exploring innovative structural possibilities in the field of reticular chemistry. Detailed structural analysis of these FKMOFs and

Received: March 29, 2024

Revised: May 31, 2024

Accepted: June 13, 2024

Published: June 20, 2024



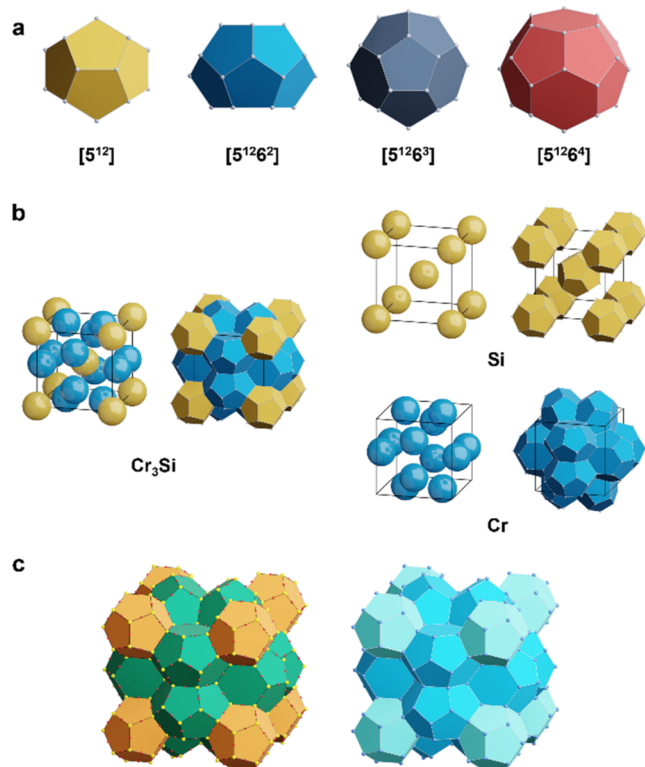


Figure 1. FK polyhedra and FK structures. (a) FK polyhedra: Pentagonal dodecahedron $[5^{12}]$ (yellow), tetradecahedron $[5^{12}6^2]$ (blue), pentadecahedron $[5^{12}6^3]$ (navy), hexadecahedron $[5^{12}6^4]$ (red). (b) Schematic illustration of Cr_3Si structure and corresponding **mep** topology with dodecahedra (yellow) and tetradecahedra (blue). (c) Examples of **mep** topology: Melanophlogite (Si, yellow spheres; O, red spheres) and clathrate type I (O, blue spheres; H omitted for clarity) from left to right. The dual net³⁵ of **mep**, known as an A15 lattice, is also popular in soft materials such as dendrimers,^{36–39} block copolymers,^{40,41} small molecules,^{42,43} giant supermolecules,^{44–46} and colloidal crystals^{47–49} (Figure S1).

their related tetrahedron-based frameworks, such as zeolites and zeolitic imidazolate frameworks (ZIFs),⁵⁶ has revealed the essential role of the T-O-T angle in **mep** topology. Importantly, adjusting the tetrahedral coordination system modifies energy landscapes, revealing new insights toward accessing other “treasure-trove” FK topologies, perhaps waiting to be discovered in MOFs.

RESULTS AND DISCUSSION

FKMOF-1 [$\text{Cd}_{23}(\text{HMTA})_{11.5}(\text{CH}_3\text{COO})_{46}(\text{H}_2\text{O})_{23}$, HMTA = hexamethylenetetramine] was synthesized by a solvothermal reaction of HMTA as a tetrahedral ligand and $\text{Cd}(\text{CH}_3\text{COO})_2$ in a mixture of *N*-methyl-2-pyrrolidone (NMP), ethanol, and water. FKMOF-1 crystallized in the $R\bar{3}c$ trigonal space group with $a = 47.909(4)$ Å and $c = 58.677(6)$ Å (Figure S2a and Table S1). Single-crystal data of FKMOF-1 were collected at the Pohang Accelerator Laboratory (PAL) in Korea. Each HMTA ligand was coordinated to four Cd(II) ions, effectively creating a tetrahedron, whereas each Cd(II) ion was axially coordinated by two HMTA ligands (Figure S3). The tetrahedra were the basic structural building units forming **mep** topology, which was based on two types of polyhedra, namely dodecahedra $[5^{12}]$ and tetradecahedra $[5^{12}6^2]$ with a ratio of 1:3 (Figure 2). This is the first reported case of **mep** topology in MOFs. The framework window sizes were 9.8 and 11.8 Å for pentagonal and hexagonal windows, respectively. The inner diameters of the dodecahedra (Figure 2b) and tetradecahedra (Figure 2c) were 17.0 and 17.7 Å, respectively, as measured from the face closest to the centroid of the polyhedron. Each dodecahedron was composed of 20 HMTA ligands and 30 Cd ions, whereas each tetradecahedron consisted of 24 HMTA ligands and 36 Cd ions. Acetates which were coordinated to Cd ion or placed in the pores balanced the charge in FKMOF-1 (Figures S3b and S4). There were five different bond angles (162, 174, 175, 176, and 180°) between a Cd ion and the two HMTA ligands (Figure S3b). The powder X-ray diffraction (PXRD) patterns of the as-synthesized FKMOF-1 matched well with the simulated pattern (Figure S5) from the single-crystal data.

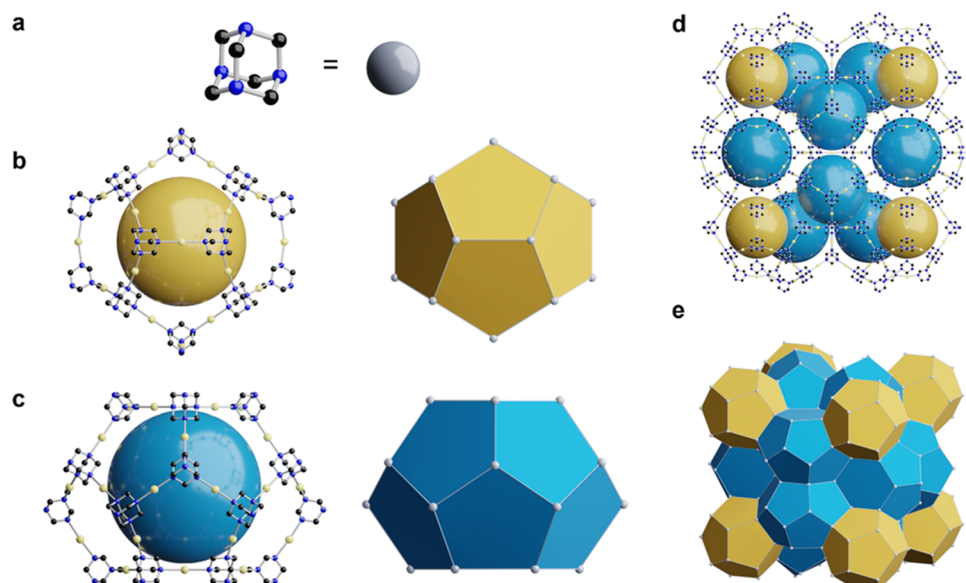


Figure 2. Structure of FKMOF-1. (a) HMTA as a simplified ball (C, black spheres; N, blue spheres). (b) Dodecahedral $[5^{12}]$ (yellow) and (c) tetradecahedral $[5^{12}6^2]$ (blue) cages with Cd (light yellow) cations. (d) A three-dimensional molecular network of **mep**-MOF, FKMOF-1. (e) FK polyhedral cage framework of FKMOF-1.

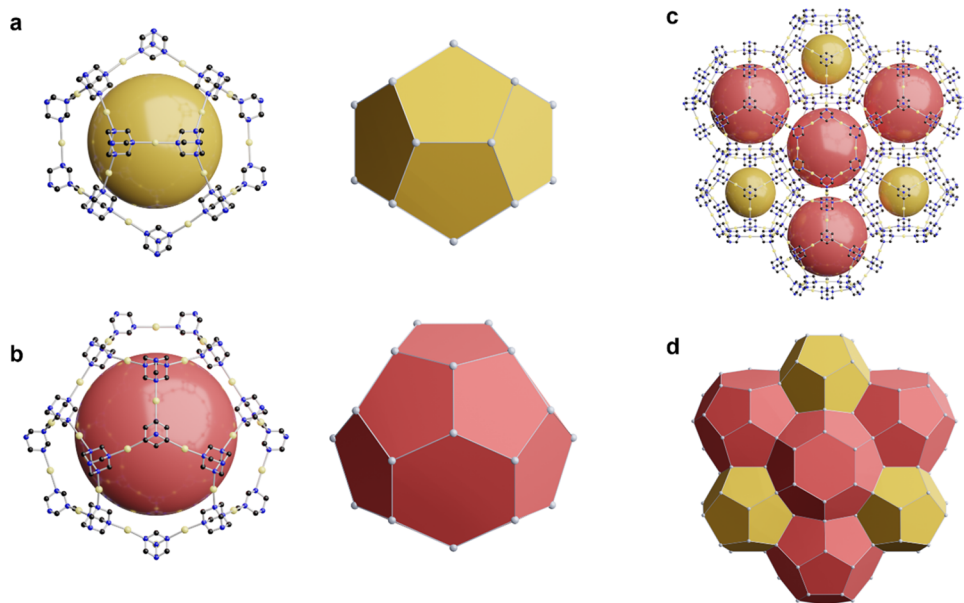


Figure 3. Structure of FKMOM-2. (a) Dodecahedral $[S^{12}]$ (yellow) and (b) hexadecahedral $[S^{12}6^4]$ (red) cages. (c) A three-dimensional molecular network of **mtn**-MOF, FKMOM-2. (d) FK polyhedral cage framework of FKMOM-2 viewed along the $[111]$ direction.

FKMOM-2 $[Cd_{17}(HMTA)_{8.5}Br_{51}\cdot(N(CH_3)_4)_{17}]$ was synthesized by a solvothermal reaction of HMTA, $CdBr_2$, and tetramethylammonium nitrate in a mixture of *N,N*-Dimethylacetamide (DMA), ethanol, and water. FKMOM-2 crystallized in the $F\bar{d}3m$ space group with $a = 48.831(6)$ Å (Figure S2b and Table S2). FKMOM-2 was constructed from dodecahedra $[S^{12}]$ and hexadecahedra $[S^{12}6^4]$ with a 2:1 ratio in **mtn** topology (Figure 3). Fang et al. previously reported an MOF structure with the same topology synthesized under different conditions using $CdCl_2$ and HMTA.⁵⁰ The dodecahedron and hexadecahedron had inner diameters of 17.4 and 21.2 Å, respectively, and framework window sizes of 10 and 10–12.4 Å, respectively (Figure 3). The packing pattern and coordination environment for Cd ions in FKMOM-2 are noticeably different (Figures S3 and S6). Each Cd site was coordinated by three Br anions (Figure S3c). To compensate charge, tetramethylammonium cations exist in FKMOM-2 framework (Figure S7). The powder X-ray diffraction patterns of the as-synthesized FKMOM-2 also matched well with the simulated pattern (Figure S8).

Several thousand intermetallic alloys are referred to as FK phases, and their space fillings are based on FK polyhedra. Such cellular topologies found in the Reticular Chemistry Structure Resource (RCSR) database are **mep**, **mtn**, **mgz-x-d**, **zra-d**, **muh**, **mur**, **sig**, **tei**, and **tep** (Table 1 and Figure S9).^{6,20,57} Especially, **mep** topology is found in compounds ranging from hard solids

to soft matter, including an efficient bubble foam, known as a counter-example to Kelvin's conjecture as the Weaire-Phelan structure.^{58–61} FKMOM-1 is the first reported case of **mep** topology in MOFs. Two examples of a zeolitic coordination network featuring **mep**-like architecture have been constructed using ligands with 5-fold symmetry, which include a pentagonal face cap.^{62,63} However, these structures indeed exhibit **mef**, not **mep** topology. To construct the FK topologies, tetrahedral units are used as basic units for FK polyhedra, as can be seen in FKMOMs and zeolites, such as melanophlogite (MEP)²² and ZSM-39 (MTN).⁶⁴ Such zeolites are based on TO_4 tetrahedra ($T = Si$ and Al) connected by oxygen to form T-O-T bridges. Various zeolite structures display characteristic T-O-T angle distributions depending on topology (Figure S10).⁶⁵ Similarly, FKMOMs and ZIFs show analogous HMTA-Cd-HMTA, and Im-Zn-Im (Im: Imidazolate) connections, respectively (Figures 4 and S3).⁵⁶ In FKMOMs, the roles for metal and linker are reversed unlike typical MOFs. HMTA acts as silicon atom and Cd ion as oxygen in zeolites. Perhaps such reversed roles are important to stabilize the T-O-T angle distribution found in FKMOM-1, necessary for **mep** topology. The reversed roles of metals and organic linkers in MOFs could provide valuable blueprints for reticular chemists seeking novel topologies. A prime example of this reversed role is evident in **she** topology in MOFs.⁶⁶ Additionally, our work contributes significantly to understanding the diversity of geometrical features and expanding the topological possibilities in MOF chemistry.^{66,67} This approach not only broadens the scope of designs but also enriches the theoretical framework necessary for pioneering new structures in MOF field.

We investigated the T-O-T angles found in zeolites, FKMOMs, and ZIFs. In zeolites, the average T-O-T angle is 148° (measured from 24 different pure silica zeolite topologies).⁶⁸ However, zeolites with pentagonal dodecahedra, such as MEP, MTN, DOH, and DDR, have significantly higher T-O-T angles (Figure S11).^{65,68} For example, MEP and MTN zeolites have T-O-T angles of $148\text{--}180$ and $168\text{--}180^\circ$, respectively, indicating that these topologies demand excep-

Table 1. Examples of Frank-Kasper phases

structure type	dual topology	space group	tiling $[S^{12}]:[S^{12}6^2]:[S^{12}6^3]:[S^{12}6^4]$
Cr_3Si	mep	$Pm\bar{3}n$	1:3:0:0
$MgCu_2$	mtn	$Fd\bar{3}m$	2:0:0:1
$MgZn_2$	mgz-x-d	$P6_3/mmc$	2:0:0:1
Zr_4Al_3	zra-d	$P6/mmm$	3:2:2:0
$Cr_{46}Fe_{54}$	sig	$P4_2/mnm$	5:8:2:0
W_6Fe_7	mur	$R\bar{3}m$	7:2:2:2
K_7Cs_6	muh	$P6_3/mmc$	7:2:2:2
$Mg_{32}(Zn, Al)_{49}$	tei	$I\bar{m}\bar{3}$	49:6:6:20

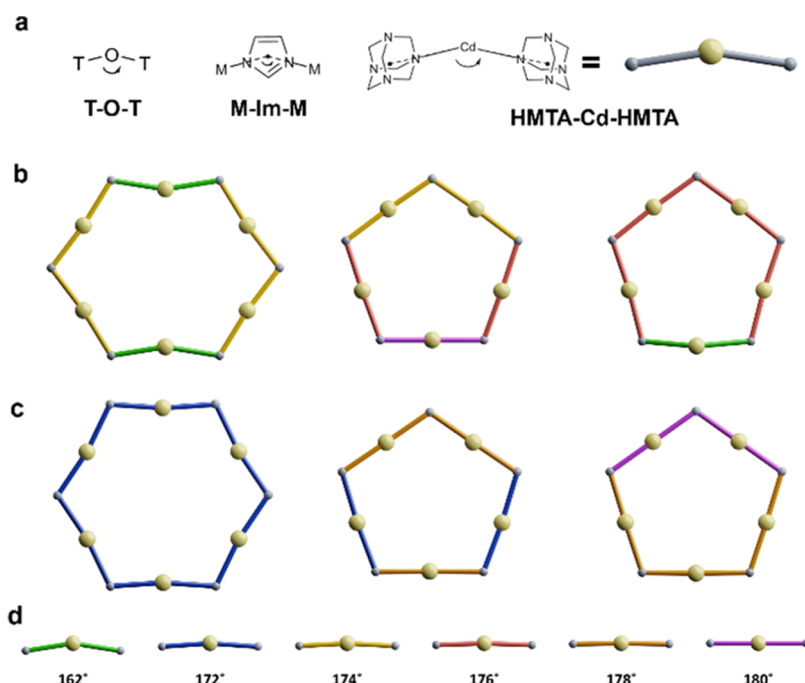


Figure 4. T-O-T bridges, polygons, and FK polyhedra in zeolites, ZIFs, FKMOM-1 and FKMOM-2. (a) T-O-T bridges formed by zeolite T-O-T, M-Im-M, and HMTA-Cd-HMTA ($T = \text{Si, Ge}$; Im = imidazolate). (b) Three types of polygons used to construct Frank–Kasper polyhedra in FKMOM-1. The left hexagon constructs tetradecahedra. The middle and right pentagons construct tetrahedra and dodecahedra, respectively. (c) Three types of polygons used to construct FK polyhedra in FKMOM-2. The left hexagon constructs hexadecahedra. The middle and right pentagons construct hexadecahedra and dodecahedra, respectively. (d) T-O-T angles found in FKMOM-1 and FKMOM-2.

tionally high T-O-T angles to form their FK polyhedra (Figure 5). The same trend can be seen in FKMOMFs. Both FKMOMFs also show high T-O-T angles, 162–180° (FKMOMF-1, **mep**) and 172–180° (FKMOMF-2, **mtn**), respectively.

In contrast, such a trend is not seen in ZIFs.^{69,70} In fact, there are no reports of **mep** or **mtn** topology in ZIFs, even though the

average T-O-T angle for ZIFs is 142°, similar to the average T-O-T angle for zeolites (148°). Interestingly, the T-O-T angle distributions for the representative ZIFs in 31 topologies are considerably lower and narrower, 133–158°, than those found in zeolites (134–180°) (Figures 5 and S12, and Table S3). To achieve **mep** and **mtn** topologies, the T-O-T angle should be close to 180° to form planar pentagons in FK polyhedra.⁷¹

We therefore hypothesize that ZIFs cannot adopt **mep** topology because of the energy penalty caused by T-O-T strain. To test our hypothesis, we calculated the energies in molecular Si–O–Si (zeolite), Zn-Im-Zn (ZIF), and HMTA-Cd-HMTA (FKMOMF) systems as a function of T-O-T angle using density functional theory (DFT)⁷² computations. Figure 6 shows the energy differences as a function of the T-O-T angle in the Si–O–Si, Zn-Im-Zn, and HMTA-Cd-HMTA systems. The potential energy curve for Si–O–Si is consistent with the previously reported data for zeolites.^{73,74} Our result for Zn-Im-Zn indicates that its energy variation is much steeper than that for the other two cases (Si–O–Si and HMTA-Cd-HMTA), which thus supports the hypothesis. When comparing the relative energy scales of Si–O–Si and Zn-Im-Zn bonds, although the trends are similar, the energy scales differ significantly, with Zn-Im-Zn exhibiting much higher energy levels. The calculations reveal that this disparity explains why zeolites can adopt **mep** topology at lower energy levels, unlike ZIFs, which cannot form this topology.

FKMOMF-1 has a moderately narrower T-O-T angle distribution (162–180°, average = 175°) than its zeolite counterpart, melanophlogite (148–180°, average = 169°). Such a difference could be due to the extra flexibility of the O-T-O angles at the Cd-HMTA-Cd node in FKMOMFs (Tables S4 and S5). All the results indicated substantial flexibility in the

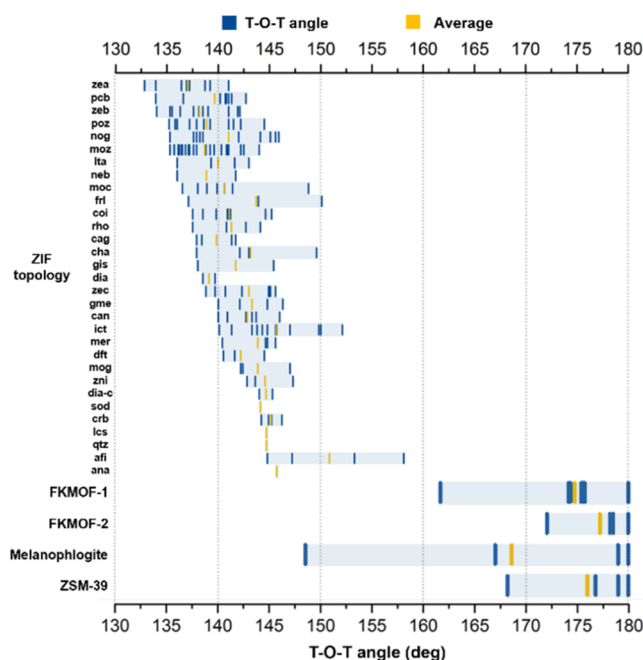


Figure 5. T-O-T angle distributions of ZIFs, FKMOMFs, and zeolites. T-O-T angle distribution of ZIFs with 31 different topologies and FKMOMF-1, FKMOMF-2, melanophlogite, and ZSM-39.

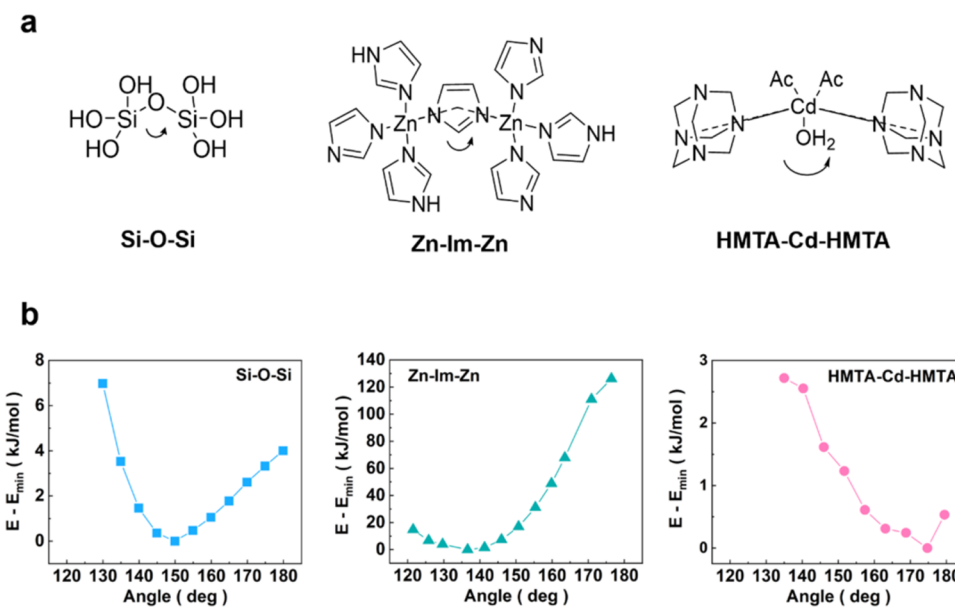


Figure 6. Theoretically calculated energy as a function of T-O-T angle. (a) Representative single-molecular clusters of T-O-T for zeolites (Si-O-Si), ZIFs (Zn-Im-Zn), and FKMOMFs (HMTA-Cd-HMTA). (b) Result plots of the energy calculations as a function of T-O-T angle for each molecular system. The left graph is for Si-O-Si, the middle one for Zn-Im-Zn, and the right one for HMTA-Cd-HMTA.

tetrahedral units, promoting the formation of **mep** topology in FKMOF-1. Thorpe et al. reported similar structural flexibility in zeolites with varying T-O-T angles.⁷⁵

Based on the T-O-T angle analysis in ZIFs and FKMOMFs, we note that the synthesis of MOFs with a wide T-O-T angle dispersion might not be a trivial task. MOFs are often assembled from rigid linkers and well-defined SBUs through strong chemical bonds, forming highly predictable topologies. For instance, MIL-100 (**moo** topology) and MIL-101 (**mtn-e** topology) are examples of MOFs that follow the underlying **mtn** topology. These MOFs are assembled using either rigid 3-connected or linear ligands, coupled with well-defined trinuclear SBU, $M_3O(COO)_6$ (Figure S13). MOFs with **mtn** topology have been characterized by narrow T-O-T angle distributions (Figure S14). Although this elegant strategy has been highly successful for building popular topologies in MOF chemistry, such an approach cannot be applicable to the present system such as **mep**, which demands a very wide T-O-T angle distribution.

There are 137 FK topological frameworks in the literature, including 29 known FK phases (Table S6).^{20,76} Additionally, Sikiric et al. have proposed 108 hypothetical FK topologies,^{30,77} which could serve as blueprints for new cellular FKMOMFs.

Among the actual and hypothetical FK topologies, we chose **mgz-x-d** (dual topology of C14 phase) and **zra-d** (clathrate type III and dual topology of Z phase) topologies for structural modeling. The FK polyhedra composition in **mgz-x-d** is identical to that of the **mtn** topology (Table S6). Additionally, the topology of **zra-d** is related to clathrate type III, distinguishing it from **mep** (type I) and **mtn** topology (type II). Moreover, the dual phases of these topologies, namely C14 and Z phases, have been realized in the assembly of soft materials,^{45,78} suggesting a potential for observation within MOF assemblies as well. Figure 7 shows two hypothetical FKMOMFs in **mgz-x-d** and **zra-d** topologies created after the geometry optimization using the Forceite module in Materials Studio 7.0.⁷⁹ The optimized structures of hypothetical FKMOMFs with **mgz-x-d** and **zra-d** topologies have hexagonal P_{63}/mmc and

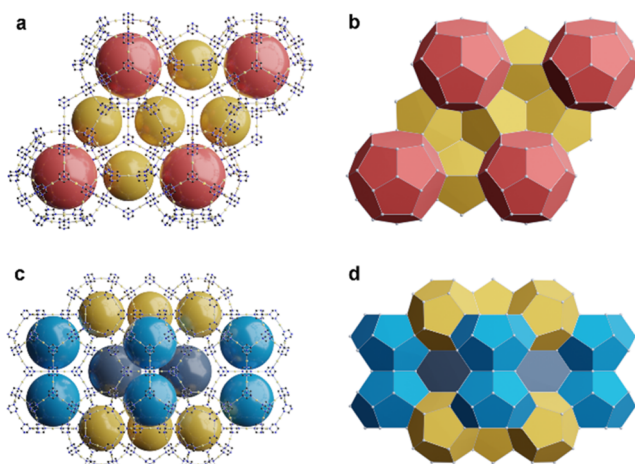


Figure 7. Structure of hypothetical FKMOMFs with **mgz-x-d** and **zra-d** topologies by structural modeling. (a) A 3D molecular network of **mgz-x-d** topology-based FKMOMF. (b) Polyhedral caged network of modeled **mgz-x-d** FKMOMF viewed along the [001] direction. (c) A 3D molecular network of **zra-d** topology-based FKMOMF. (d) Polyhedral caged network of modeled **zra-d** FKMOMF viewed along the [120] direction.

$P6/mmm$ space groups with parameters $a = 35.0680 \text{ \AA}$, $c = 57.3912 \text{ \AA}$ and $a = 34.4925 \text{ \AA}$, $c = 35.1747 \text{ \AA}$, respectively. The hypothetical FKMOMFs with **mgz-x-d** and **zra-d** topologies exhibited T-O-T angle distributions similar to those in FKMOF-2 (Figure S15). However, their O-T-O angles deviated more from the ideal tetrahedral geometry than those observed in the synthesized FKMOF-1 and FKMOF-2 (Table S7). Although the **mgz-x-d** and **zra-d** topologies have not yet been synthesized, further synthetic efforts are necessary to achieve new FK topologies.

CONCLUSIONS

We report the first MOF with **mep** topology (FKMOF-1), together with another MOF with **mtn** topology (FKMOF-2). Both topologies are related to FK structures, providing an

important structural clue to the building of new series of cellular MOFs. Detailed analysis of the T-O-T angle distribution revealed that FK polyhedra with pentagonal faces demand high T-O-T angles. Further analysis of zeolites and ZIFs also confirmed that the T-O-T angle is crucial to accessing **mep** topology. Notably, the wide range of T-O-T angles in FKMOF-1 promoted **mep** topology, which is an important structural feature unachievable in ZIFs. Significantly, the modulation of the tetrahedral coordination system alters the energy landscapes, thereby facilitating the formation of more MOFs with FK polyhedral structures. Actual and hypothetical FK topologies can be utilized as blueprints for constructing various cellular MOFs for emerging applications.

■ ASSOCIATED CONTENT

Supporting Information

The Supporting Information is available free of charge at <https://pubs.acs.org/doi/10.1021/jacsau.4c00285>.

Materials and general procedures; detailed experimental and computational methods; characterization of FKMOFs including ^1H NMR, PXRD, and SCXRD; measurements of structural information ([PDF](#))
FKMOF-1 ([CIF](#))
FKMOF-2 ([CIF](#))
Models for hypothetical FKMOFs ([ZIP](#))

Accession Codes

CCDC 1847765 (FKMOF-1) and 1487207 (FKMOF-2) contains the supporting crystallographic data for this paper. These data can be obtained free of charge via www.ccdc.cam.ac.uk/data_request/cif, or by emailing data_request@ccdc.cam.ac.uk, or by contacting The Cambridge Crystallographic Data Centre, 12 Union Road, Cambridge CB2 1EZ, U.K.; fax: + 44 1223 336033.

■ AUTHOR INFORMATION

Corresponding Authors

Sung June Cho – Department of Chemical Engineering, Chonnam National University, Gwangju 61186, Republic of Korea; orcid.org/0000-0002-0030-9409; Email: sjcho@chonnam.ac.kr

Noejung Park – Center for Multidimensional Carbon Materials, Institute for Basic Science, Ulsan 44919, Republic of Korea; Department of Physics, Ulsan National Institute of Science and Technology, Ulsan 44919, Republic of Korea; orcid.org/0000-0002-2359-0635; Email: noejung@unist.ac.kr

Wonyoung Choe – Department of Chemistry, Ulsan National Institute of Science and Technology, Ulsan 44919, Republic of Korea; Graduate School of Carbon Neutrality and Graduate School of Artificial Intelligence, Ulsan National Institute of Science and Technology, Ulsan 44919, Republic of Korea; orcid.org/0000-0003-0957-1187; Email: choe@unist.ac.kr

Authors

Soochan Lee – Department of Chemistry, Ulsan National Institute of Science and Technology, Ulsan 44919, Republic of Korea

Sungmin Lee – Department of Chemistry, Ulsan National Institute of Science and Technology, Ulsan 44919, Republic of Korea

Yuna Kwak – Department of Chemistry, Ulsan National Institute of Science and Technology, Ulsan 44919, Republic of Korea

Masood Yousaf – Center for Multidimensional Carbon Materials, Institute for Basic Science, Ulsan 44919, Republic of Korea

Eunchan Cho – Department of Chemistry, Ulsan National Institute of Science and Technology, Ulsan 44919, Republic of Korea

Hoi Ri Moon – Department of Chemistry and Nanoscience, Ewha Womans University, Seoul 03760, Republic of Korea; orcid.org/0000-0002-6967-894X

Complete contact information is available at:

<https://pubs.acs.org/10.1021/jacsau.4c00285>

Author Contributions

○ S.L. and S.L. contributed equally to this work. CRediT: **Soochan Lee** conceptualization, data curation, formal analysis, investigation, methodology, writing-original draft, writing-review & editing; **Sungmin Lee** data curation, formal analysis, investigation, methodology, writing-original draft, writing-review & editing; **Yuna Kwak** formal analysis, investigation, writing-original draft, writing-review & editing; **Masood Yousaf** data curation, formal analysis, software, validation, writing-original draft, writing-review & editing; **Eunchan Cho** investigation, visualization, writing-review & editing; **Hoi Ri Moon** investigation, validation, writing-original draft, writing-review & editing; **Sung June Cho** data curation, formal analysis, investigation, validation, writing-original draft, writing-review & editing; **Noejung Park** formal analysis, investigation, validation, writing-original draft, writing-review & editing; **Wonyoung Choe** conceptualization, funding acquisition, investigation, project administration, supervision, validation, writing-original draft, writing-review & editing.

Notes

The authors declare no competing financial interest.

■ ACKNOWLEDGMENTS

This work was financially supported by National Research Foundation of Korea (NRF-2021M3I3A1084909, RS-2023-00279793, RS-2023-00218799 and RS-2023-00208825). M.Y. acknowledges the financial support from Institute for Basic Science (IBS-R019-D1). X-ray diffraction experiments using synchrotron radiation were performed at the PAL in Korea for beamline use (2014-third-2D-024 and 2018-first-2D-030).

■ REFERENCES

- (1) Zhou, H.-C.; Long, J. R.; Yaghi, O. M. Introduction to Metal–Organic Frameworks. *Chem. Rev.* **2012**, *112* (2), 673–674.
- (2) Moghadam, P. Z.; Li, A.; Wiggin, S. B.; Tao, A.; Maloney, A. G. P.; Wood, P. A.; Ward, S. C.; Fairen-Jimenez, D. Development of a Cambridge Structural Database Subset: A Collection of Metal–Organic Frameworks for Past, Present, and Future. *Chem. Mater.* **2017**, *29* (7), 2618–2625.
- (3) Freund, R.; Canossa, S.; Cohen, S. M.; Yan, W.; Deng, H.; Guillerm, V.; Eddaoudi, M.; Madden, D. G.; Fairen-Jimenez, D.; Lyu, H.; Macreadie, L. K.; Ji, Z.; Zhang, Y.; Wang, B.; Haase, F.; Wöll, C.; Zaremba, O.; Andreo, J.; Wuttke, S.; Diercks, C. S. 25 Years of Reticular Chemistry. *Angew. Chem., Int. Ed.* **2021**, *60* (45), 23946–23974.
- (4) Kalmutzki, M. J.; Hanikel, N.; Yaghi, O. M. Secondary Building Units as the Turning Point in the Development of the Reticular Chemistry of MOFs. *Sci. Adv.* **2018**, *4* (10), eaat9180.

- (5) Lu, W.; Wei, Z.; Gu, Z.-Y.; Liu, T.-F.; Park, J.; Park, J.; Tian, J.; Zhang, M.; Zhang, Q.; Gentle Iii, T.; Bosch, M.; Zhou, H.-C. Tuning the Structure and Function of Metal–Organic Frameworks via Linker Design. *Chem. Soc. Rev.* **2014**, *43* (16), 5561–5593.
- (6) O’Keeffe, M.; Peskov, M. A.; Ramsden, S. J.; Yaghi, O. M. The Reticular Chemistry Structure Resource (RCSR) Database of, and Symbols for, Crystal Nets. *Acc. Chem. Res.* **2008**, *41* (12), 1782–1789.
- (7) O’Keeffe, M. Design of MOFs and Intellectual Content in Reticular Chemistry: A Personal View. *Chem. Soc. Rev.* **2009**, *38* (5), 1215–1217, DOI: 10.1039/b802802h.
- (8) Tranchemontagne, D. J.; Mendoza-Cortés, J. L.; O’Keeffe, M.; Yaghi, O. M. Secondary Building Units, Nets and Bonding in the Chemistry of Metal–Organic Frameworks. *Chem. Soc. Rev.* **2009**, *38* (5), 1257–1283, DOI: 10.1039/b817735j.
- (9) Jiang, H.; Alezi, D.; Eddaoudi, M. E. A reticular chemistry guide for the design of periodic solids. *Nat. Rev. Mater.* **2021**, *6* (6), 466–487.
- (10) Guillerm, V.; Kim, D.; Eubank, J. F.; Luebke, R.; Liu, X.; Adil, K.; Lah, M. S.; Eddaoudi, M. A Supermolecular Building Approach for the Design and Construction of Metal–Organic Frameworks. *Chem. Soc. Rev.* **2014**, *43* (16), 6141–6172.
- (11) Kim, D.; Liu, X.; Lah, M. S. Topology Analysis of Metal–Organic Frameworks Based on Metal–Organic Polyhedra as Secondary or Tertiary Building Units. *Inorg. Chem. Front.* **2015**, *2* (4), 336–360.
- (12) Khobotov-Bakishev, A.; Hernández-López, L.; von Baeckmann, C.; Albalad, J.; Carné-Sánchez, A.; Maspoch, D. Metal–Organic Polyhedra as Building Blocks for Porous Extended Networks. *Adv. Sci.* **2022**, *9* (11), No. 2104753.
- (13) Guillerm, V.; Eddaoudi, M. The Importance of Highly Connected Building Units in Reticular Chemistry: Thoughtful Design of Metal–Organic Frameworks. *Acc. Chem. Res.* **2021**, *54* (17), 3298–3312.
- (14) Li, P.; Vermeulen, N. A.; Mallikas, C. D.; Gómez-Gualdrón, D. A.; Howarth, A. J.; Mehdi, B. L.; Dohnalkova, A.; Browning, N. D.; O’Keeffe, M.; Farha, O. K. Bottom-up construction of a superstructure in a porous uranium-organic crystal. *Science* **2017**, *356* (6338), 624–627.
- (15) Barsukova, M.; Sapianik, A.; Guillerm, V.; Shkurenko, A.; Shaikh, A. C.; Parvatkar, P.; Bhatt, P. M.; Bonneau, M.; Alhaji, A.; Shekhah, O.; Balestra, S. R. G.; Semino, R.; Maurin, G.; Eddaoudi, M. Face-directed assembly of tailored isoreticular MOFs using centring structure-directing agents. *Nat. Synth.* **2024**, *3* (1), 33–46.
- (16) O’Keeffe, M. Crystal Structures as Periodic Foams and Vice Versa. In *Foams and Emulsions*; Sadoc, J. F.; Rivier, N., Eds.; Springer Netherlands: Dordrecht, 1999; pp. 403–422.
- (17) Frank, F. C.; Kasper, J. S. Complex Alloy Structures Regarded as Sphere Packings. I. Definitions and Basic Principles. *Acta Crystallogr.* **1958**, *11* (3), 184–190.
- (18) Frank, F. C.; Kasper, J. S. Complex Alloy Structures Regarded as Sphere Packings. II. Analysis and Classification of Representative Structures. *Acta Crystallogr.* **1959**, *12* (7), 483–499.
- (19) Bonneau, C.; O’Keeffe, M. Intermetallic Crystal Structures as Foams. Beyond Frank–Kasper. *Inorg. Chem.* **2015**, *54* (3), 808–814.
- (20) Sikirić, M. D.; Delgado-Friedrichs, O.; Deza, M. Space Fullerenes: A Computer Search for New Frank–Kasper Structures. *Acta Crystallogr., Sect. A: Found. Crystallogr.* **2010**, *66* (5), 602–615.
- (21) Kamb, B. A Clathrate Crystalline Form of Silica. *Science* **1965**, *148* (3667), 232–234.
- (22) Gies, H. Studies on Clathrasils. III.*: Crystal Structure of Melanophlogite, a Natural Clathrate Compound of Silica**. *Z. Kristallogr. - Cryst. Mater.* **1983**, *164* (3–4), 247–257.
- (23) Momma, K.; Ikeda, T.; Nishikubo, K.; Takahashi, N.; Honma, C.; Takada, M.; Furukawa, Y.; Nagase, T.; Kudoh, Y. New Silica Clathrate Minerals That Are Isostructural with Natural Gas Hydrates. *Nat. Commun.* **2011**, *2* (1), No. 196.
- (24) Sloan, E. D. Fundamental Principles and Applications of Natural Gas Hydrates. *Nature* **2003**, *426* (6964), 353–359.
- (25) Kirchner, M. T.; Boese, R.; Billups, W. E.; Norman, L. R. Gas Hydrate Single-Crystal Structure Analyses. *J. Am. Chem. Soc.* **2004**, *126* (30), 9407–9412.
- (26) Pouchard, M.; Cros, C. The Early Development of Inorganic Clathrates. In *The Physics and Chemistry of Inorganic Clathrates*; Nolas, G. S., Ed.; Springer Netherlands: Dordrecht, 2014; Vol. 199, pp 1–33.
- (27) Kasper, J. S.; Hagenmuller, P.; Pouchard, M.; Cros, C. Clathrate Structure of Silicon $\text{Na}_8 \text{Si}_{46}$ and $\text{Na}_x \text{Si}_{136}$ ($x < 11$). *Science* **1965**, *150* (3704), 1713–1714.
- (28) Aydemir, U.; Akselrud, L.; Carrillo-Cabrera, W.; Candolfi, C.; Oeschler, N.; Baitinger, M.; Steglich, F.; Grin, Y. BaGe₅: A New Type of Intermetallic Clathrate. *J. Am. Chem. Soc.* **2010**, *132* (32), 10984–10985.
- (29) He, Y.; Sui, F.; Kauzlarich, S. M.; Galli, G. Si-Based Earth Abundant Clathrates for Solar Energy Conversion. *Energy Environ. Sci.* **2014**, *7* (8), 2598–2602.
- (30) Sui, F.; He, H.; Bobev, S.; Zhao, J.; Osterloh, F. E.; Kauzlarich, S. M. Synthesis, Structure, Thermoelectric Properties, and Band Gaps of Alkali Metal Containing Type I Clathrates: $\text{A}_8 \text{Ga}_8 \text{Si}_{38}$ ($\text{A} = \text{K}, \text{Rb}, \text{Cs}$) and $\text{K}_8 \text{Al}_8 \text{Si}_{38}$. *Chem. Mater.* **2015**, *27* (8), 2812–2820.
- (31) Luo, M.-B.; Chen, L.-J.; Huang, S.-L.; Zhou, X.; Chen, E.-X.; Lin, Q. Zeolite Analogues Based on Oxysulfidometalate Supertetrahedral Clusters via Coulombic Interactions. *Inorg. Chem. Front.* **2023**, *10*, 3224–3229.
- (32) Klarreich, E. G. Foams and Honeycombs: For centuries, the precise architecture of soap foams has been a source of wonder to children and a challenge to mathematicians. *Am. Sci.* **2000**, *88*, 152–161.
- (33) Boomsma, K.; Poulikakos, D.; Ventikos, Y. Simulations of flow through open cell metal foams using an idealized periodic cell structures. *Int. J. Heat Fluid Flow* **2003**, *24*, 825–834, DOI: 10.1016/j.ijheatfluidflow.2003.08.002.
- (34) Ball, P. Beijing Bubbles. *Nature* **2007**, *448* (7151), 256.
- (35) Chen, Y.; Takeya, S.; Sum, A. K. Topological Dual and Extended Relations between Networks of Clathrate Hydrates and Frank–Kasper Phases. *Nat. Commun.* **2023**, *14* (1), No. 596.
- (36) Hudson, S. D.; Jung, H.-T.; Percec, V.; Cho, W.-D.; Johansson, G.; Ungar, G.; Balagurusamy, V. S. K. Direct Visualization of Individual Cylindrical and Spherical Supramolecular Dendrimers. *Science* **1997**, *278* (5337), 449–452.
- (37) Percec, V.; Cho, W.-D.; Möller, M.; Prokhorova, S. A.; Ungar, G.; Yeardley, D. J. P. Design and Structural Analysis of the First Spherical Monodendron Self-Organizable in a Cubic Lattice. *J. Am. Chem. Soc.* **2000**, *122* (17), 4249–4250.
- (38) Ungar, G.; Liu, Y.; Zeng, X.; Percec, V.; Cho, W.-D. Giant Supramolecular Liquid Crystal Lattice. *Science* **2003**, *299* (5610), 1208–1211.
- (39) Percec, V.; Peterca, M.; Dulcey, A. E.; Imam, M. R.; Hudson, S. D.; Nummelin, S.; Adelman, P.; Heiney, P. A. Hollow Spherical Supramolecular Dendrimers. *J. Am. Chem. Soc.* **2008**, *130* (39), 13079–13094.
- (40) Bates, M. W.; Lequieu, J.; Barbon, S. M.; Lewis, R. M.; Delaney, K. T.; Anastasaki, A.; Hawker, C. J.; Fredrickson, G. H.; Bates, C. M. Stability of the A15 Phase in Diblock Copolymer Melts. *Proc. Natl. Acad. Sci. U.S.A.* **2019**, *116* (27), 13194–13199.
- (41) Watanabe, M.; Asai, Y.; Suzuki, J.; Takano, A.; Matsushita, Y. Frank–Kasper A15 Phase Formed in AB_n Block-Graft Copolymers with Large Numbers of Graft Chains. *Macromolecules* **2020**, *53* (22), 10217–10224.
- (42) Montis, R.; Fusaro, L.; Falqui, A.; Hursthorne, M. B.; Tumanov, N.; Coles, S. J.; Threlfall, T. L.; Horton, P. N.; Sougrat, R.; Lafontaine, A.; Coquerel, G.; Rae, A. D. Complex Structures Arising from the Self-Assembly of a Simple Organic Salt. *Nature* **2021**, *590* (7845), 275–278.
- (43) Kim, S. A.; Jeong, K.-J.; Yethiraj, A.; Mahanthappa, M. K. Low-Symmetry Sphere Packings of Simple Surfactant Micelles Induced by Ionic Sphericity. *Proc. Natl. Acad. Sci. U.S.A.* **2017**, *114* (16), 4072–4077.
- (44) Huang, M.; Hsu, C.-H.; Wang, J.; Mei, S.; Dong, X.; Li, Y.; Li, M.; Liu, H.; Zhang, W.; Aida, T.; Zhang, W.-B.; Yue, K.; Cheng, S. Z. D. Selective Assemblies of Giant Tetrahedra via Precisely Controlled Positional Interactions. *Science* **2015**, *348* (6233), 424–428.

- (45) Su, Z.; Hsu, C.-H.; Gong, Z.; Feng, X.; Huang, J.; Zhang, R.; Wang, Y.; Mao, J.; Wesdemiotis, C.; Li, T.; Seifert, S.; Zhang, W.; Aida, T.; Huang, M.; Cheng, S. Z. D. Identification of a Frank–Kasper Z Phase from Shape Amphiphile Self-Assembly. *Nat. Chem.* **2019**, *11* (10), 899–905.
- (46) Chen, C.; Poppe, M.; Poppe, S.; Wagner, M.; Tschierske, C.; Liu, F. Tetrahedral liquid-crystalline networks: an A1S-like Frank-Kasper Phase based on rod-packing. *Angew. Chem., Int. Ed.* **2022**, *61* (27), No. e202203447.
- (47) Lin, H.; Lee, S.; Sun, L.; Spellings, M.; Engel, M.; Glotzer, S. C.; Mirkin, C. A. Clathrate Colloidal Crystals. *Science* **2017**, *355* (6328), 931–935.
- (48) Girard, M.; Wang, S.; Du, J. S.; Das, A.; Huang, Z.; Dravid, V. P.; Lee, B.; Mirkin, C. A.; De La Cruz, M. O. Particle Analogs of Electrons in Colloidal Crystals. *Science* **2019**, *364* (6446), 1174–1178.
- (49) Wang, S.; Lee, S.; Du, J. S.; Partridge, B. E.; Cheng, H. F.; Zhou, W.; Dravid, V. P.; Lee, B.; Glotzer, S. C.; Mirkin, C. A. The Emergence of Valency in Colloidal Crystals through Electron Equivalents. *Nat. Mater.* **2022**, *21* (5), 580–587.
- (50) Fang, Q.; Zhu, G.; Xue, M.; Sun, J.; Wei, Y.; Qiu, S.; Xu, R. A Metal–Organic Framework with the Zeolite MTN Topology Containing Large Cages of Volume 2.5 nm³. *Angew. Chem., Int. Ed.* **2005**, *44* (25), 3845–3848.
- (51) Férey, G.; Serre, C.; Mellot-Draznieks, C.; Millange, F.; Surblé, S.; Dutour, J.; Margiolaki, I. A Hybrid Solid with Giant Pores Prepared by a Combination of Targeted Chemistry, Simulation, and Powder Diffraction. *Angew. Chem., Int. Ed.* **2004**, *43* (46), 6296–6301.
- (52) Férey, G.; Mellot-Draznieks, C.; Serre, C.; Millange, F.; Dutour, J.; Surblé, S.; Margiolaki, I. A Chromium Terephthalate-Based Solid with Unusually Large Pore Volumes and Surface Area. *Science* **2005**, *309* (5743), 2040–2042.
- (53) Park, Y. K.; Choi, S. B.; Kim, H.; Kim, K.; Won, B.; Choi, K.; Choi, J.; Ahn, W.; Won, N.; Kim, S.; Jung, D. H.; Choi, S.; Kim, G.; Cha, S.; Jhon, Y. H.; Yang, J. K.; Kim, J. Crystal Structure and Guest Uptake of a Mesoporous Metal–Organic Framework Containing Cages of 3.9 and 4.7 nm in Diameter. *Angew. Chem., Int. Ed.* **2007**, *46* (43), 8230–8233.
- (54) Kang, Y.; Wang, F.; Zhang, J.; Bu, X. Luminescent MTN -Type Cluster–Organic Framework with 2.6 nm Cages. *J. Am. Chem. Soc.* **2012**, *134* (43), 17881–17884.
- (55) Thorp-Greenwood, F. L.; Kulak, A. N.; Hardie, M. J. Three-Dimensional Silver-Dabco Coordination Polymers with Zeolitic or Three-Connected Topology. *Cryst. Growth Des.* **2014**, *14* (11), 5361–5365.
- (56) Park, K. S.; Ni, Z.; Côté, A. P.; Choi, J. Y.; Huang, R.; Uribe-Romo, F. J.; Chae, H. K.; O’Keeffe, M.; Yaghi, O. M. Exceptional Chemical and Thermal Stability of Zeolitic Imidazolate Frameworks. *Proc. Natl. Acad. Sci. U.S.A.* **2006**, *103* (27), 10186–10191.
- (57) O’Keeffe, M.; Adams, G. B.; Sankey, O. F. Duals of Frank-Kasper Structures as C, Si and Ge Clathrates: Energetics and Structure. *Philos. Mag. Lett.* **1998**, *78* (1), 21–28.
- (58) Thomson, W. On the division of space with minimum partitional area. *Acta Math.* **1887**, *11*, 121–134.
- (59) Gray, J. Parsimonious Polyhedra. *Nature* **1994**, *367*, 598–599.
- (60) Weaire, D.; Phelan, R. A Counter-Example to Kelvin’s Conjecture on Minimal Surfaces. *Philos. Mag. Lett.* **1994**, *69* (2), 107–110.
- (61) Gabrielli, R.; Meagher, A. J.; Weaire, D.; Brakke, K. A.; Hutzler, S. An Experimental Realization of the Weaire–Phelan Structure in Monodisperse Liquid Foam. *Philos. Mag. Lett.* **2012**, *92* (1), 1–6.
- (62) Bacsa, J.; Less, R. J.; Skelton, H. E.; Soracevic, Z.; Steiner, A.; Wilson, T. C.; Wood, P. T.; Wright, D. S. Assembly of the First Fullerene-Type Metal–Organic Frameworks Using a Planar Five-Fold Coordination Node. *Angew. Chem., Int. Ed.* **2011**, *50* (36), 8279–8282.
- (63) Zhang, W.; Wang, K.; Li, J.; Lin, Z.; Song, S.; Huang, S.; Liu, Y.; Nie, F.; Zhang, Q. Stabilization of the Pentazolate Anion in a Zeolitic Architecture with Na₂₀N₆₀ and Na₂₄N₆₀ Nanocages. *Angew. Chem., Int. Ed.* **2018**, *57* (10), 2592–2595.
- (64) Schlenker, J. L.; Dwyer, F. G.; Jenkins, E. E.; Rohrbaugh, W. J.; Kokotailo, G. T.; Meier, W. M. Crystal Structure of a Synthetic High Silica Zeolite—ZSM-39. *Nature* **1981**, *294* (5839), 340–342.
- (65) Baerlocher, C.; McCusker, L. Database of zeolite structures 2017 <http://www.izastructure.org/databases/>.
- (66) Gómez-Gualdrón, D. A.; Cólón, Y. J.; Zhang, X.; Wang, T. C.; Chen, Y.-S.; Hupp, J. T.; Yıldırım, T.; Farha, O. K.; Zhang, J.; Snurr, R. Q. Evaluating Topologically Diverse Metal–Organic Frameworks for Cryo-Adsorbed Hydrogen Storage. *Energy Environ. Sci.* **2016**, *9* (10), 3279–3289.
- (67) Moosavi, S. M.; Nandy, A.; Jablonka, K. M.; Ongari, D.; Janet, J. P.; Boyd, P. G.; Lee, Y.; Smit, B.; Kulik, H. J. Understanding the Diversity of the Metal-Organic Framework Ecosystem. *Nat. Commun.* **2020**, *11* (1), No. 4068.
- (68) Wragg, D. S.; Morris, R. E.; Burton, A. W. Pure Silica Zeolite-Type Frameworks: A Structural Analysis. *Chem. Mater.* **2008**, *20* (4), 1561–1570.
- (69) Noh, K.; Lee, J.; Kim, J. Compositions and Structures of Zeolitic Imidazolate Frameworks. *Isr. J. Chem.* **2018**, *58* (9–10), 1075–1088.
- (70) Lee, S.; Nam, D.; Yang, D. C.; Choe, W. Unveiling Hidden Zeolitic Imidazolate Frameworks Guided by Intuition-Based Geometrical Factors. *Small* **2023**, *19* (15), No. 2300036.
- (71) O’Keeffe, M. Tetrahedral Frameworks TX₂ with T–X–T Angle = 180°. *Mater. Res. Bull.* **2006**, *41* (5), 911–915.
- (72) Hohenberg, P.; Kohn, W. Inhomogeneous Electron Gas. *Phys. Rev.* **1964**, *136* (3B), B864–B871.
- (73) Kamakoti, P.; Barckholtz, T. A. Role of Germanium in the Formation of Double Four Rings in Zeolites. *J. Phys. Chem. C* **2007**, *111* (9), 3575–3583.
- (74) Sastre, G.; Corma, A. Predicting Structural Feasibility of Silica and Germania Zeolites. *J. Phys. Chem. C* **2010**, *114* (3), 1667–1673.
- (75) Sartbaeva, A.; Wells, S. A.; Treacy, M. M. J.; Thorpe, M. F. The Flexibility Window in Zeolites. *Nat. Mater.* **2006**, *5* (12), 962–965.
- (76) Liu, X.-Y.; Yan, X.-Y.; Liu, Y.; Qu, H.; Wang, Y.; Wang, J.; Guo, Q.-Y.; Lei, H.; Li, X.-H.; Bian, F.; Cao, X.-Y.; Zhang, R.; Wang, Y.; Huang, M.; Lin, Z.; Meijer, E. W.; Aida, T.; Kong, X.; Cheng, S. Z. D. Self-Assembled Soft Alloy with Frank–Kasper Phases beyond Metals. *Nat. Mater.* **2024**, *23* (4), 570–576.
- (77) Sikirić, M. D.; Deza, M. Space Fullerenes: Computer Search for New Frank–Kasper Structures II. *Struct. Chem.* **2012**, *23* (4), 1103–1114.
- (78) Kim, K.; Schulze, M. W.; Arora, A.; Lewis, R. M.; Hillmyer, M. A.; Dorfman, K. D.; Bates, F. S. Thermal Processing of Diblock Copolymer Melts Mimics Metallurgy. *Science* **2017**, *356* (6337), 520–523.
- (79) Materials Studio v7.0; Accelrys Software Inc.: San Diego, CA 92121, USA.